

Electronic origin of variable denitrosylation kinetics from isostructural {FeNO}⁷ complexes: X-ray crystal structure of [Fe(oetap)(NO)][†]

D. Scott Bohle,^{*a} Peter Debrunner,^b Jeffrey P. Fitzgerald,^c Bernhard Hansert,^a Chen-Hsiung Hung^a and Andrew J. Thomson^d

^a Department of Chemistry, University of Wyoming, Laramie, Wyoming 82071-3838, USA

^b Department of Physics, University of Illinois Urbana-Champaign, Illinois 61801, USA

^c Department of Chemistry, United States Naval Academy, Annapolis, Maryland 21402, USA

^d School of Chemical Sciences, University of East Anglia, Norwich, UK NR4 7TJ

In contrast to the nitrosyl derivative of iron(II) octaethylporphyrin [Fe(oep)(NO)], the isostructural octaethyltetraazaporphyrin complex [Fe(oetap)(NO)] exhibits fast ligand-promoted nitric oxide dissociation in the presence of pyridine and *N*-methylimidazole.

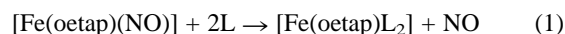
Iron(II) nitric oxide complexes of phthalocyanines have been known for over 30 years.^{1–3} Although they are closely related to intensively studied porphyrin compounds,⁴ they are in general not well characterized and very little is known about their solution reaction chemistry because of their poor solubility. We have begun to systematically explore the reactivity of iron(II) porphyrin nitrosyls and now extend our studies to include soluble iron(II) octaethyltetraazaporphyrins, [Fe(oetap)].^{5,6} Herein we describe: (i) the synthesis of the nitrosyl derivative of iron(II) octaethyltetraazaporphyrin [Fe(oetap)(NO)] and its characterization by IR, EPR, Mössbauer spectroscopies, electrochemistry and elemental analysis; (ii) the structure of [Fe(oetap)(NO)] as determined by single-crystal X-ray diffraction; (iii) the comparison of the spectroscopic properties of [Fe(oetap)(NO)] and [Fe(oep)(NO)]; and (iv) the markedly different dissociation kinetics of nitric oxide from these two compounds promoted by pyridine and *N*-methylimidazole. Together these results illustrate the effect of the macrocyclic ligand on the properties and reactivities of ferrous nitrosyl complexes.

The iron(II) nitrosyl complexes [Fe(oep)(NO)] and [Fe(oetap)(NO)] are readily prepared under reductive nitrosylation conditions by treating [FeLCl] with nitric oxide in the presence of excess methanol and 2,6-dimethylpyridine.^{7‡} Their characterisation data, Table 1, are typical for paramagnetic five-coordinate iron(II) nitrosyl complexes in which the nitric oxide ligand adopts a bent geometry and the electronic structure is best described as a delocalized {FeNO}⁷ configuration.⁸ The most pronounced difference between [Fe(oep)(NO)] and [Fe(oetap)(NO)] is the potential of the first oxidation couple, {FeNO}^{6–}{FeNO}⁷, which increases by 350 mV for [Fe(oetap)(NO)], indicating the more electron-withdrawing nature of the nitrogen atoms for the tetraaza derivative compared to the CH units in [Fe(oep)(NO)]. In addition, the larger quadrupolar

splitting observed in the Mössbauer spectrum as well as the unusually clear anisotropy and hyperfine coupling observed near $g = 2.00$ for the low-temperature EPR spectra of [Fe(oetap)(NO)], is indicative of there being a larger ligand field in the [Fe(oetap)(NO)] complex. In the case of the ¹⁴N¹⁵O derivative two triplets are observed and assigned in the EPR spectrum as $g_z = 2.000$ with $a_z = 17.77$ G, and $g_y = 2.029$, $a_y = 16.03$ G. The third signal, g_x , is presumably part of the low-field shoulder of the overall manifold. The EPR spectra of [Fe(oep)(NO)] and other five-coordinate nitrosyl adducts of iron(II) porphyrins, in general do not exhibit such clear anisotropic signals with well resolved hyperfine coupling in their low-temperature spectra.⁹ The decreased core size for the oetap ligand is the best explanation for these macrocyclic effects. In order to rule out aggregation as the origin of these spectroscopic features spectra with tenfold greater and smaller concentrations were measured under identical conditions; the resulting spectra retain all of these features.

Direct support for the interpretation of these spectroscopic results is found in the single-crystal X-ray diffraction structure of [Fe(oetap)(NO)].[§] Unlike other related disordered structures, the bent nitrosyl ligand in this complex adopts a single geometry, Fig. 1, with the nitrosyl oriented away from the four ethyl groups on the same face of the macrocycle. In spite of the smaller core size of the tetraazaporphyrin, the {FeNO}⁷ fragment in this complex adopts a very typical geometry in terms of the Fe–N–O bond angle [143.7(4)°], the iron displacement from the macrocycle [0.308(1) Å], and the dihedral angle N(3)–Fe–N(9)–O(1) [39.6(6)°].¹⁰

Considering the similarity in the structural and spectroscopic features of [Fe(oetap)(NO)] and [Fe(oep)(NO)], it is surprising to find that nitric oxide dissociation from the former is four orders of magnitude faster when they are treated with coordinating ligands such as pyridine and *N*-methylimidazole, cf. Table 1, eqn. (1).



The products from these reactions [Fe(oetap)L₂]^{5,6} form isobestically with the same kinetics in both the presence and absence of dioxygen. However, as shown in Fig. 2, nitric oxide

Table 1 Summary of physical and kinetic data for [Fe(oep)(NO)] and [Fe(oetap)(NO)]

Compound	$\nu(\text{NO})^a/\text{cm}^{-1}$	E_z^b/mV	g_{iso}	$a(^{14}\text{N})/\text{G}$	Mössbauer data ^d /mm s ⁻¹		Added ligand L	[L]/m	$k_{\text{obs}}^e/\text{s}^{-1}$
					Δ	δ			
[Fe(oep)(NO)]	1672	390	2.05	18.0	1.258(1)	0.348(1)	<i>N</i> -mim py	6.3 6.0	$3.8(1) \times 10^{-5}$ $2.2(1) \times 10^{-5}$
[Fe(oetap)(NO)]	1666	733	1.99	17.0	1.951(1)	0.209(1)	<i>N</i> -mim py	6.3 6.0	0.148(2) 0.072(1)

^a KBr pellet. ^b Potentials in mV vs. Ag⁺/Ag in dichloromethane solution with 0.1 M NBu₄PF₆ as supporting electrolyte on a platinum-button working electrode. ^c Room-temp. EPR spectra measured in toluene solution. ^d At 100 K. ^e Pseudo-first-order rate constants for the rate of denitrosylation in 1 : 1 toluene–ligand solution at 25 °C.

dissociation from [Fe(oetap)(NO)] exhibits saturation behaviour and at high concentrations of *N*-mim reaches a limiting maximum rate of 0.148 s⁻¹. These observations suggest a mechanism which involves rapid equilibrium binding of axial ligand to [Fe(oetap)(NO)] followed by a rate-determining loss of nitric oxide from the six-coordinate intermediate. Thus the observed rates under saturation conditions correspond to nitric oxide dissociation rates as was found for [Fe(obtpp)(NO)].

Nitric oxide is now recognized as an ubiquitous intercellular messenger whose predominant and most well characterized signal transduction pathway involves the up-regulation of soluble guanylate cyclase (sGC) by binding to its iron(II) haem centre.¹¹ The denitrosylative down-regulation of this key enzyme remains poorly understood, with simple nitric oxide dissociation being frequently discounted due to the generally

observed slow rate.¹² Several cases where facile ligand-promoted loss of nitric oxide are now known^{10,13} and the factors which control these fundamental transformations are under investigation. The isostructural pair of complexes in this study are significant in that although they have almost identical steric constraints on axial ligand binding, they exhibit dramatic differences in reactivity. These results are clearly directly due to the marked differences in electronic structures of these compounds as shown in their Mössbauer and EPR spectra. Although an exact determination of the electronic structures of these species will require exacting levels of theory, it is clear that coordination of axial ligands populates orbitals with net Fe–NO antibonding character. The challenge is to determine which factors, under direct control of the polypeptide–haem–NO interaction, can also increase the lability of nitric oxide when bound to haem proteins such as sGC.

We gratefully acknowledge support from the Department of Energy (DE-FCO2-91ER) Burroughs–Wellcome Foundation for a Hitchings–Elion Fellowship (D. S. B.), the Henry and Camille Dreyfus Foundation for a Teacher–Scholar award (D. S. B.) and the EPSRC and BBSRC for support for the Centre for Metalloprotein Spectroscopy and Biology at UEA (A. J. T.).

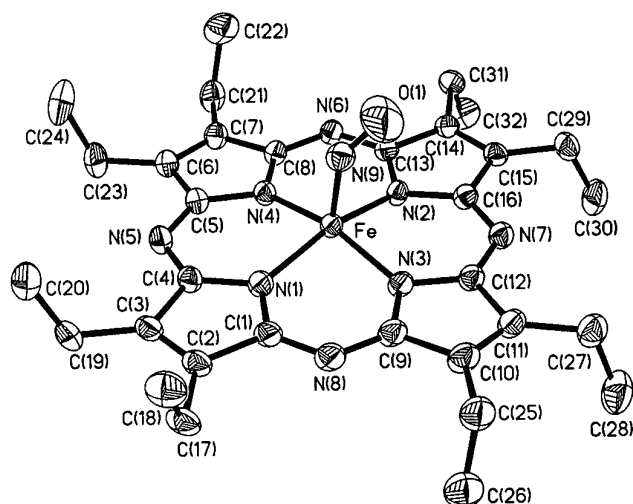


Fig. 1 Molecular structure of [Fe(oetap)(NO)], with hydrogen atoms omitted for clarity. Important bond lengths (Å) and angles (°): Fe(1)–N(1–4) 1.922–1.941(3), Fe(1)–N(9) 1.721(4), N(9)–O(1) 1.155(5); Fe(1)–N(9)–O(1) 143.7(4).

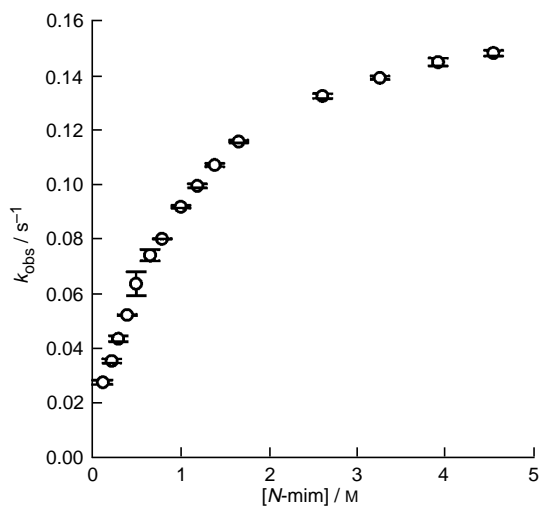


Fig. 2 Observed rate of denitrosylation under pseudo-first-order conditions for [Fe(oetap)(NO)] as a function of *N*-methylimidazole concentration. Conditions: [Fe(oetap)(NO)]_{initial} = 1.67 × 10⁻⁵ M, *T* = 25 °C, solvent mixture of *N*-methylimidazole with toluene and iodobenzene (19% volume).

Footnotes

† Abbreviations: oep = dianion of 2,3,7,8,12,13,17,18-octaethylporphyrin; oetap = dianion of 2,3,7,8,12,13,17,18-octaethyl-5,10,15,20-tetraazaporphyrin; obtpp = dianion of 2,3,7,8,12,13,17,18-octabromo-5,10,15,20-tetraazaporphyrin, *N*-mim = *N*-methylimidazole.

‡ Characterisation data for [Fe(oetap)(NO)]: UV–VIS [CHCl₃, λ nm(log ε)] 316(4.57), 350(4.49), 590(4.49); IR(KBr, cm⁻¹) ν(¹⁵NNO) = 1638.4 cm⁻¹; Anal. Calc. for C₃₂H₄₀FeN₉O, C, 61.73; H, 6.48; N, 20.25; Found: C, 61.71; H, 6.49; N, 20.14%.

§ Crystal data: [Fe(oetap)(NO)], C₃₂H₄₀FeN₉O, *M* = 622.6, triclinic, space group *P*1 (no. 2), *a* = 10.378(2), *b* = 10.541(3), *c* = 14.290(3) Å, α = 79.36, β = 88.63(3), γ = 80.07(3)°, *U* = 1513.3(5) Å³, *Z* = 2, *D*_c = 1.366 Mg m⁻³, λ = 0.71073 Å, μ = 0.541 mm⁻¹, *F*(000) = 658, *T* = 298 K. Data were collected on a Siemens P4 diffractometer for 2 < θ < 27.5°. The structure was solved by direct and Fourier methods and refined by least squares against *F*² to *R*1 = 0.0471 (*wR*2 = 0.0609) for 3870 unique intensity data with *I* > 6σ(*I*). Atomic coordinates, bond lengths and angles, and thermal parameters have been deposited at the Cambridge Crystallographic Data Centre (CCDC). See Information for Authors, Issue No. 1. Any request to the CCDC for this material should quote the full literature citation and the reference number 182/307.

References

- G. Sartori and C. Ercolani, *Ricorca Sci.*, 1963, **33**, 323.
- C. Ercolani, A. M. Paoletti, G. Pennesi and G. Rossi, *J. Chem. Soc., Dalton Trans.*, 1991, 1317.
- C. Ercolani and C. Neri, *J. Chem. Soc. A*, 1967, 1715.
- T. Yoshimura, *Bull. Chem. Soc. Jpn.*, 1991, **64**, 2819.
- J. P. Fitzgerald, B. S. Haggerty, A. L. Rheingold, L. May and G. A. Brewer, *Inorg. Chem.*, 1992, **31**, 2006.
- J. P. Fitzgerald, G. Yap, A. L. Rheingold, C. T. Brewer, L. May and G. A. Brewer, *J. Chem. Soc., Dalton Trans.*, 1996, 1249.
- B. B. Wayland and L. W. Olson, *J. Am. Chem. Soc.*, 1974, **96**, 6037.
- R. D. Feltham and J. Enemark, *Coord. Chem. Rev.*, 1974, **13**, 339.
- T. Yoshimura, *J. Inorg. Biochem.*, 1983, **18**, 263.
- D. S. Bohle and C.-H. Hung, *J. Am. Chem. Soc.*, 1995, **117**, 9584 and references therein.
- L. J. Ignarro, *Biochem. Soc. Trans.*, 1992, **20**, 465.
- J. R. Stone and M. A. Marletta, *Biochemistry*, 1994, **33**, 5636.
- J. M. C. Ribeiro, J. M. H. Hazzard, R. H. Nussenzveig, D. E. Champagne and F. A. Walker, *Science*, 1993, **260**, 539.

Received, 8th October 1996; Com. 6/06880D